CrossMark

## ORIGINAL PAPER

# Mechanism of TEMPO-oxidized cellulose nanofibril film reinforcement with poly(acrylamide)

**Takanori Kurihara · Akira Isogai**

**Abstract** 2,2,6,6-Tetramethylpiperidine-1-oxyl (TEMPO)-oxidized cellulose nanofibrils (TOCNs) and poly(acrylamide) (PAM) with sodium carboxylate groups (TOCN-COONa and PAM-COONa, respectively) were converted to TOCN and PAM with protonated carboxyl groups (TOCN-COOH and PAM-COOH, respectively). Transparent and flexible PAM-COOH/TOCN-COOH, PAM-COONa/TOCN-COOH, and PAM-COOH/TOCN-COONa composite films were prepared by mixing aqueous PAM-COOH or PAM-COONa solutions and aqueous TOCN-COOH or TOCN-COONa dispersions with various PAM/TOCN weight ratios, and successive casting/drying of the mixtures. In all cases, the Young's modulus and tensile strength of the composite film were highest when the PAM content of the composite film was in the range 10–25 %. PAM therefore has the potential to reinforce TOCN films, irrespective of the sodium carboxylate groups or protonated carboxyl groups of TOCN or PAM. Although the FT-IR spectra of the PAM-COOH/TOCN-COOH composite films with various PAM/TOCN weight ratios indicated the formation of hydrogen bonds between PAM-COOH and TOCN-COOH, the formation of these hydrogen bonds could not explain the reinforcing effect achieved by PAM addition to TOCN-COOH. Because the TOCN elements form nematic-ordered or self-aligned domain structures in aqueous dispersions, PAM molecules at the corresponding PAM contents are probably present around the boundary regions of TOCN domains, and fill or cover the defects present between the TOCN domains.

**Keywords** TEMPO · Cellulose nanofibril · Poly(acrylamide) · Counter ion · Tensile properties · Composite film

## Introduction

The catalytic oxidation of plant celluloses with 2,2,6,6-tetramethylpiperidine-1-oxy (TEMPO) radicals under aqueous conditions is one of the most effective pretreatments for the preparation of nanocelluloses, with reduced energy consumption during the mechanical disintegration process of the cellulose fibers in water (Saito et al. 2007; Isogai et al. 2011; Klemm et al., 2011; Isogai 2013). The characteristic points of TEMPO-oxidized cellulose nanofibrils (TOCNs) are as follows. (1) When papermaking-grade bleached wood celluloses are used, the obtained TOCNs have homogeneous widths of $\sim 3$ nm and high aspect ratios, >100 (Saito et al. 2007). (2) Sodium carboxylate

T. Kurihara · A. Isogai (✉)
Graduate School of Agricultural and Life Sciences, The University of Tokyo, 1-1-1 Yayoi, Bunkyo-ku, Tokyo 113-8657, Japan
e-mail: aisogai@mail.ecc.u-tokyo.ac.jp

T. Kurihara
R&D Company, Harima Chemicals Inc., 671-4 Mizuashi, Noguchi-cho, Kakogawa, Hyogo 675-0019, Japan

groups are abundantly and regularly present on the TOCN surfaces (Isogai et al. 2011). (3) TOCNs are nanodispersed in water, forming self-aligned and nematic-ordered domain structures (Saito et al. 2011). TOCN films are therefore expected to be have applications as new bio-based nanomaterials with good mechanical and oxygen-barrier properties (Fukuzumi et al. 2009; Isogai et al. 2011). If TOCNs can be replaced by an inexpensive conventional polymer, while giving mechanical, optical, oxygen-barrier, and thermal properties similar to those of 100 % TOCNs, less expensive materials for use in various high-tech fields could be produced. Because TOCN is nanodispersible in water, it is advantageous for TOCNs to contain water-soluble polymers or water-nanodispersible nanoclays to achieve homogeneous distribution of TOCN elements in matrix polymers or inorganic nanoparticles (Henriksson et al. 2008; Johnson et al. 2009; Sehaqui et al. 2010, 2011; Liu et al. 2011; Endo et al. 2013; Wu et al. 2012, 2014).

Poly(acrylamides) (PAMs) are water-soluble synthetic polymers; they have been widely used as dry paper-strength and retention aids in papermaking, and the methods for controlling their molecular weights, cationic/anionic charge densities, and degrees of cross-linking are already well established. When aqueous solutions of PAMs with various molecular weights, charge densities, and degrees of cross-linking are mixed with aqueous TOCN dispersions with various PAM/TOCN weight ratios, the PAM/TOCN composite films prepared by casting and drying aqueous PAM/TOCN mixtures with a weight ratio of 25/75 have better mechanical properties than those of 100 % TOCN films. PAM molecules therefore reinforce TOCN matrix film when the molecular weights, charge densities, and degrees of cross-linking of the PAMs are adequately controlled (Kurihara and Isogai 2014, 2015).

TOCNs have considerable amounts of sodium C6-carboxylate groups (or sodium glucuronosyl units) on the fibril surfaces, and therefore TOCNs can be completely and efficiently dispersed at the individual nanofibril level in water (Saito et al. 2007; Isogai et al. 2011). The abundant sodium carboxylate groups on TOCN surfaces are exchangeable with protons and other metal ions by simple ion-exchange treatments (Fujisawa et al. 2011; Homma et al. 2013; Fukuzumi et al. 2013; Shimizu et al. 2013, 2014a, b). All TOCNs and PAMs used in previous studies for the preparation of PAM/TOCN composite films contained sodium

carboxylate groups (Kurihara and Isogai 2014, 2015). However, if TOCNs or PAMs with protonated carboxyl groups instead of sodium carboxylate groups are used, the mechanical properties are expected to be improved by formation of hydrogen bonds between the TOCN surfaces and PAM molecules in PAM/TOCN composite films. This is because the protonated carboxyl groups of TOCNs can form hydrogen bonds with the protonated carboxyl groups/hydroxyl groups of TOCNs and acrylamide groups of PAMs.

In this study, TOCN and PAM samples with protonated carboxyl groups, i.e., TOCN-COOH and PAM-COOH, were prepared from TOCN-COONa and PAM-COONa, respectively, by ion-exchange treatment. PAM/TOCN composite films with protonated carboxyl groups, i.e., (PAM/TOCN)-H films, were prepared by mixing aqueous PAM-COOH solutions and aqueous TOCN-COOH dispersions with various PAM/TOCN weight ratios. Their tensile properties were evaluated in terms of the PAM content. The mechanism of the improvement of the tensile properties of the TOCN film by incorporating 10–25 % PAM is discussed on the basis of the obtained results. (PAM/TOCN)-Na films were prepared from PAM-COONa and TOCN-COONa; other films were also prepared, and their properties were evaluated as references.

## Experimental

### Materials

Fibrous TEMPO-oxidized cellulose (TOC) was prepared from a commercial softwood bleached kraft pulp (SBKP) (Nippon Paper Co., Ltd., Tokyo, Japan) by TEMPO/NaBr/NaClO oxidation in water at pH 10, according to a previously reported method, and subsequent post-oxidation with $NaClO_2$ in water at pH 4.8 for 2 days (Shinoda et al. 2012; Kurihara and Isogai 2014, 2015). The obtained $NaClO_2$-oxidized TOC had a carboxylate content of 1.30 mmol/g. PAM-COONa with an anionic charge density of $-1.02$ meq/g, a weight-average molecular mass ($M_w$) of 2 060 000 g/mol, and a polydispersity index of 5.7 was prepared from acrylamide and acrylic acid (9:1 molar ratio) according to a previously reported method (Kurihara and Isogai 2015). Other reagents and solvents were obtained from Wako Pure Chemical Industries, Ltd. (Osaka, Japan) and used as received.

## Preparation of aqueous TOCN-COONa and TOCN-COOH dispersions

An aqueous 0.15 % w/v TOCN-COONa dispersion was prepared by mechanical disintegration of a NaClO$_2$-oxidzied TOC/water slurry, using blender-type and ultrasonic homogenizers (Excel Auto ED-4, Nissei, Japan and US-300T, Nissei, Japan, respectively) (Kurihara and Isogai 2015). 1 M HCl was added to the 0.15 % TOCN-COONa dispersion under magnetic stirring to set the pH at ~2, and the mixture was stirred at room temperature for 30 min. The originally flowable TOCN-COONa dispersion turned to a non-flowable gel as a result of protonation of the TOCN carboxyl groups. The gel was sequentially washed with 0.01 M HCl and distilled water by repeated centrifugation at 12,000g. The gel was subjected to sonication for 1 min to prepare a 0.15 % w/v transparent and flowable TOCN-COOH/water dispersion (Fujisawa et al. 2011).

## Preparation of aqueous PAM-COONa and PAM-COOH solutions

1 M HCl was added to a 1 % w/w aqueous PAM-COONa solution (100 mL) to set the pH at ~2. Acetone (200 mL) was added to the solution and the mixture was stirred at room temperature for 30 min. The mixture was allowed to stand for an additional 30 min, and the white precipitate was collected by centrifugation and washed thoroughly with acetone. The precipitate was dissolved in water and precipitated again in acetone, and this sequence was repeated twice to prepare PAM-COOH. Finally, the PAM-COOH was dissolved in water and recovered as a solid by freeze-drying and subsequent vacuum-drying. The weight recovery ratio of PAM-COOH was more than 98 %, and the $M_w$ of PAM-COOH was the same as that of the original PAM-COONa.

## Preparation of PAM/TOCN composite films

A 0.15 % PAM solution and an aqueous 0.15 % TOCN dispersion were mixed in various PAM/TOCN weight ratios. PAM-COONa/TOCN-COONa and PAM-COOH/TOCN-COOH composite films with a PAM/TOCN weight ratio of, for example, 25/75 are denoted by (PAM/TOCN = 25/75)-Na and (PAM/TOCN = 25/75)-H, respectively. The pHs of the aqueous mixtures of (PAM/TOCN)-Na and (PAM/TOCN)-

H were ~7 and ~4, respectively. After stirring for at least 30 min, the mixture was degassed under vacuum for a short time, and poured into a poly(styrene) petri dish, followed by drying in a ventilated oven, without a forced air flow, at 40 °C for 2 days. The obtained self-standing PAM/TOCN composite films of thickness ~10 μm were conditioned at 23 °C and 50 % relative humidity (RH) for more than 1 day before analyses.

## Analyses

Colloidal titration was used to determine the electrical charge densities of the PAMs and TOCNs, using a Mütek PCD-04 streaming current detector (Germany) with either 0.0025 N poly(diallyldimethylammonium chloride) or potassium poly(vinyl sulfate) (Chen et al. 2003). The thicknesses, moisture contents at 23 °C and 50 % RH, light transmittance spectra, and tensile properties of composite films of thickness ~10 μm were obtained using the methods described in previous papers (Kurihara and Isogai 2014, 2015). At least ten film specimens were examined for each sample in the tensile tests. The viscosity-average degrees of polymerization ($DP_v$) of SBKP, NaClO$_2$-treated TOC, and TOCNs were measured at 20 °C using 0.5 M copper ethylenediamine as the solvent and a Cannon–Fenske-type capillary viscometer. The intrinsic viscosities of SBKP, NaClO$_2$-treated TOC, and TOCNs were converted to $DP_v$ values using the Mark–Houwink–Sakurada equation (Hiraoki et al. 2015). The sodium ion contents of the aqueous PAM/TOCN mixtures were determined using inductively coupled plasma optical emission spectroscopy (Agilent 720-ES). The analytical conditions were as follows: sample concentration 0.05–0.15 % w/w, injection volume 500 μL, radio frequency power 1.2 kW, plasma gas flow rate 15 L/min, auxiliary gas flow rate 1.5 L/min, and nebulizer gas flow rate 1.5 L/min. The analytical line of sodium at 588.995 nm was selected, and the sodium concentration was calculated using a calibration curve.

## Results and discussion

### Preparation of aqueous TOCN-COOH dispersions and aqueous PAM-COOH solutions

Self-standing TOCN-COOH and PAM-COOH films were prepared from aqueous TOCN-COOH dispersions

and PAM-COOH solutions by casting and drying, after ion-exchange treatment from sodium carboxylates to protonated carboxyl groups. The aqueous TOCN-COOH dispersions were prepared according to a previously reported method (Fujisawa et al. 2011). The $DP_v$ values of SBKP, NaClO$_2$-oxidized TOC, TOCN-COONa, and TOCN-COOH were 2100, 360, 270, and 210, respectively. The $DP_v$ value of the original SBKP therefore clearly decreased, primarily during TEMPO-mediated oxidation in water at pH 10. The $DP_v$ value of TOC was as low as $\sim$200 when post-oxidation with NaClO$_2$ was not performed on TOC (Shinoda et al. 2012). The mechanical disintegration of the NaClO$_2$-oxidzied TOC in water caused an additional decrease in the $DP_v$. The $DP_v$ value of TOCN-COOH was further decreased, because an additional sonication treatment was applied to the protonated TOCN gel in water to obtain a flowable TOCN-COOH/water dispersion.

The FT-IR spectra of the self-standing TOCN-COONa, TOCN-COOH, PAM-COONa, and PAM-COOH films are shown in Fig. 1. The spectra confirm that almost all the sodium carboxylate groups in TOCN-COONa were converted to protonated carboxyl groups by the ion-exchange treatment (Fujisawa et al. 2011). In the case of PAM-COONa, the C=O stretching band appeared at 1563 cm$^{-1}$, and this band disappeared from the PAM-COOH spectrum. Although the C=O band of protonated carboxyls in PAM-COOH overlapped with those of amide C=O bands at $\sim$1680 cm$^{-1}$, the disappearance of the absorption band at 1563 cm$^{-1}$ proved almost

complete conversion of the sodium carboxylate groups of PAM-COONa to protonated carboxyls in PAM-COOH by the ion-exchange treatment used in this study.

## Fundamental properties of PAM/TOCN composite films

(PAM/TOCN)-H composite films were prepared by mixing aqueous PAM-COOH solutions and aqueous TOCN-COOH dispersions with various PAM/TOCN weight ratios, and subsequent casting and drying of the mixtures. Preparation of (PAM/TOCN)-Na composite films has been reported in previous papers (Kurihara and Isogai 2014, 2015), and the data were used as references. All the (PAM/TOCN)-H films had high transparencies, with $\sim$90 % light transmittances at 600 nm, and exhibited clear interference fringe patterns, showing that the PAM-COOH and TOCN-COOH components are present homogeneously in the composite films, without detectable agglomeration, and the film surfaces are sufficiently smooth (Fig. 2) (Takahashi et al. 2009). The (PAM/TOCN)-Na film with a PAM/TOCN weight ratio of 50/50 had a lower light transmittance pattern than the others, and showed no interference fringe pattern, indicating the formation of agglomerates or heterogeneous distribution of the two components in the film.

The moisture contents and densities of the PAM/TOCN composite films are shown in Fig. 3. Because the sodium carboxylate groups of the (PAM/TOCN)-



**Fig. 1** FT-IR spectra of TOCN-COONa, TOCN-COOH, PAM-COONa, and PAM-COOH films
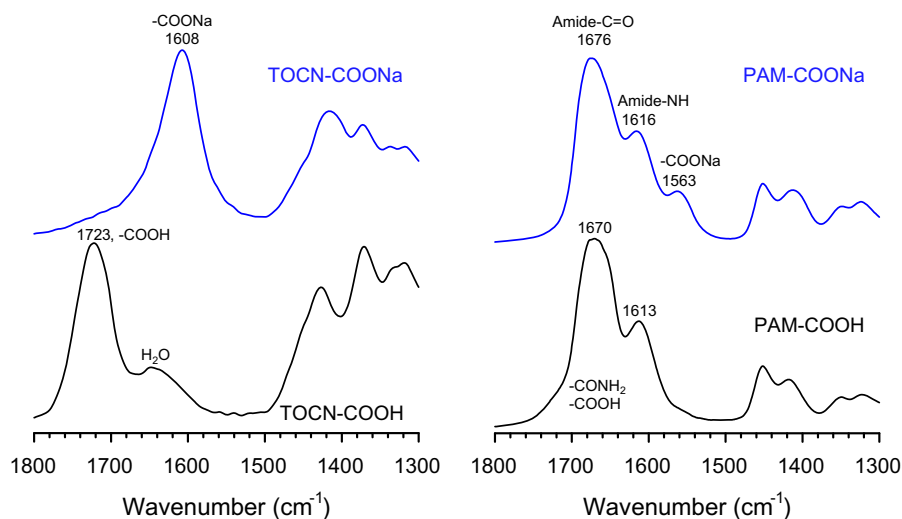
Na films are hydrophilic and cannot form hydrogen bonds with PAM or TOCN, each film had a 2.5–3.4 % higher moisture content at 23 °C and 50 % RH than that of the (PAM/TOCN)-H film at the same PAM content. The protonated carboxyl groups in the (PAM/TOCN)-H films therefore probably form hydrogen bonds with the amide groups of PAM and carboxyl/hydroxyl groups of TOCN in the composite films, and are less hydrophilic. The moisture content increased with increasing PAM content in the composite films, because of the hydrophilic nature of the abundant amide groups of amorphous PAM molecules.
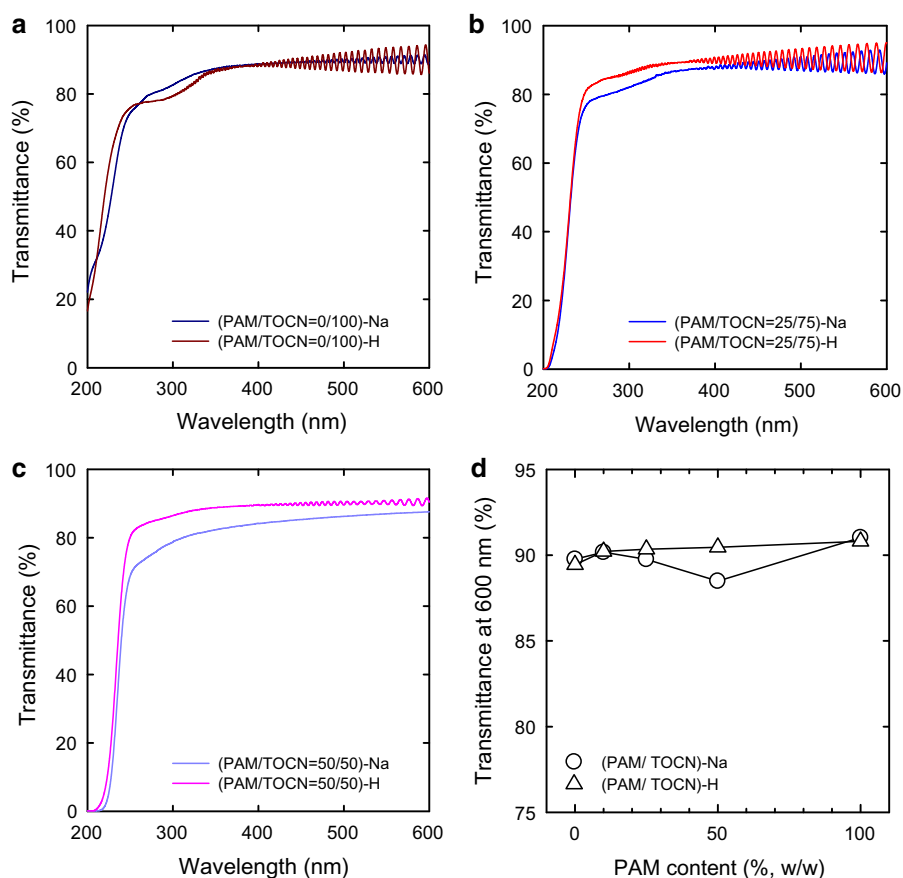
The densities of the (PAM/TOCN)-Na and (PAM/TOCN)-H films at the same PAM content differed slightly from each other, and the film density decreased almost linearly with increasing PAM content for both composite films. These film densities were determined for the composite films conditioned at 23 °C and 50 % RH, and therefore adsorbed water on the films was taken into account when measuring the film weights and thicknesses. The film densities

shown in Fig. 3b are consistent with those calculated from the weight ratios of the three components and their densities: adsorbed water (1.000 g/cm$^3$), TOCN (1.514 g/cm$^3$), and PAM (1.384 g/cm$^3$). The densities of 100 % TOCN and PAM films were used in the calculations.

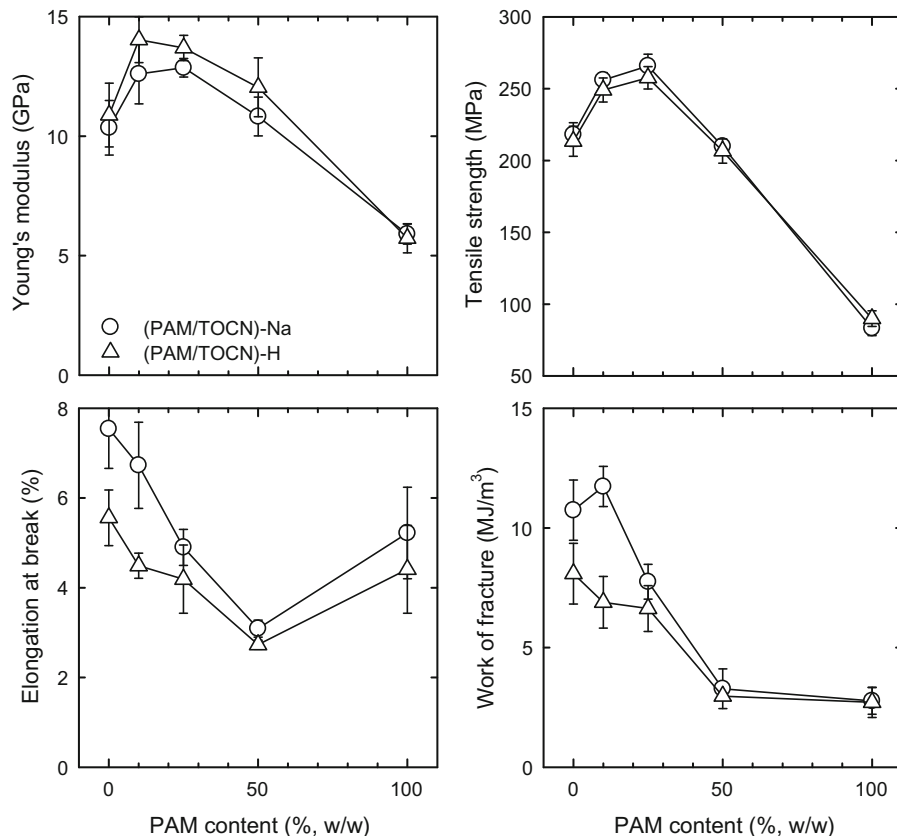## Mechanical properties of PAM/TOCN composite films

Figure 4 shows the Young's moduli, tensile strengths, elongations at break, and works of fracture for the composite films with various PAM contents. The (PAM/TOCN)-Na and (PAM/TOCN)-H films had similar patterns of Young's moduli, tensile strengths, and yield stresses (data not shown) with respect to the PAM content; they had maximum values at 10–25 % PAM contents, irrespective of the carboxyl counter ion (i.e., either protonated carboxyl or sodium carboxylate groups) and moisture contents of the (PAM/TOCN)-Na and (PAM/TOCN)-H films.



**Fig. 2** Light transmittance spectra of (PAM/TOCN)-Na and (PAM/TOCN)-H composite films with PAM/TOCN weight ratios of 0/100 (**a**), 25/75 (**b**), and 50/50 (**c**), and light transmittances (%) at 600 nm of composite films (**d**)
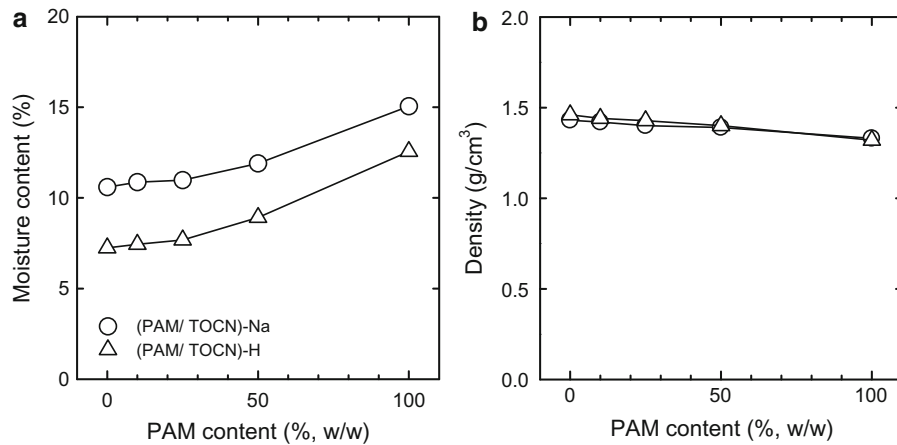
**Fig. 3** Moisture contents (**a**) and densities (**b**) of (PAM/TOCN)-Na and (PAM/TOCN)-H composite films with various PAM/TOCN weight ratios
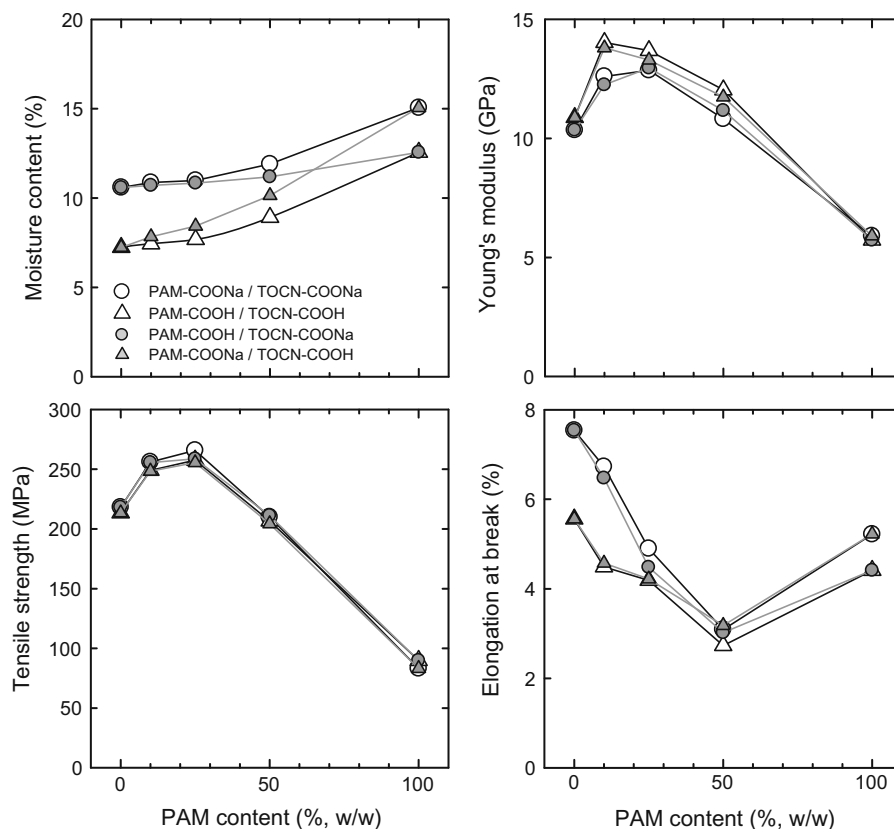


**Fig. 4** Tensile properties of (PAM/TOCN)-Na and (PAM/TOCN)-H composite films with various PAM/TOCN weight ratios

The values of elongation at break and work of fracture seem to have characteristic patterns that depend on the PAM content; this is difficult to interpret at present. The elongation decreased with increasing PAM content up to 50 %, and then increased at 100 % PAM content for both the (PAM/

**Fig. 5** Tensile properties of PAM-COONa/TOCN-COONa, PAM-COOH/TOCN-COOH, PAM-COOH/TOCN-COONa, and PAM-COONa/TOCN-COOH composite films with various PAM/TOCN weight ratios

TOCN)-Na and (PAM/TOCN)-H films. These elongation patterns with respect to PAM content did not correlate with those of either the Young's modulus or tensile strength. The elongations of the (PAM/TOCN)-Na films were larger than those of the (PAM/TOCN)-H films at 0–10 % PAM contents. This can be explained in terms of the higher moisture contents of the former films; the presence of moisture between the TOCN components in the films probably make the films ductile (Fujisawa et al. 2011). The large works of fracture for the (PAM/TOCN)-Na films at 0–10 % PAM contents are also explicable in terms of the large elongations at break, because of the high moisture contents compared with those of the (PAM/TOCN)-H films.

We initially anticipated that the (PAM/TOCN)-H composite films would have higher Young's moduli and tensile strengths, but lower elongations at break than those of the (PAM/TOCN)-Na films. This is because the protonated carboxyl groups abundantly present on the TOCN-COOH surfaces can form hydrogen bonds with the abundant amide groups in the PAM molecules and hydroxyl/carboxyl groups present on the TOCN-COOH surfaces, whereas sodium carboxylate groups cannot form hydrogen bonds. However, the results in Fig. 4 show that there were no significant differences in Young's modulus or tensile strength between the (PAM/TOCN)-H and (PAM/TOCN)-Na films at the same PAM content, indicating that the hydrogen bonds formed between TOCN-COOH and PAM had almost no influence on the mechanical properties of the (PAM/TOCN)-H composite films. The details are discussed later.

Properties of PAM/TOCN composite films with different counter ions between PAM and TOCN

PAM-COOH/TOCN-COONa and PAM-COONa/TOCN-COOH composite films with different PAM/
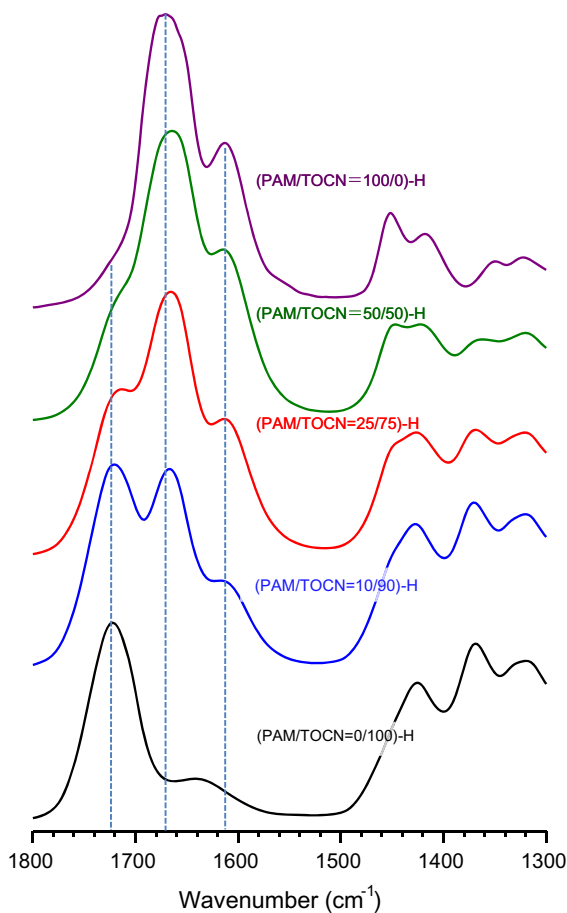
**Fig. 6** FT-IR spectra of (PAM/TOCN)-H composite films with various PAM/TOCN weight ratios

TOCN weight ratios were prepared, and their moisture contents and tensile properties were compared with those obtained for the (PAM/TOCN)-Na and (PAM/TOCN)-H composite films, shown in Figs. 3 and 4. The moisture contents of the PAM-COOH/TOCN-COONa and PAM-COONa/TOCN-COOH composite films were well explained in terms of an addition rule regarding the moisture content of each component (Fig. 5); the moisture content of the composite film depends on the mixing weight ratio of the two components.

The patterns of the Young's moduli, tensile strengths, and elongations at break of the PAM-COOH/TOCN-COONa films at different PAM contents were close to those of the (PAM/TOCN)-Na films, and those of the PAM-COONa/TOCN-COOH films were nearly the same as those of the (PAM/TOCN)-H films. Moreover, no significant differences

in Young's modulus or tensile strength were observed between all the composite films at the same PAM content. These results show that the counter ion of TOCN or PAM, i.e., either sodium carboxylate groups or protonated carboxyl groups, has no significant influence on the patterns of the Young's moduli or tensile strengths with changing PAM content. The PAM content, rather than the counter ion of the carboxyl groups of TOCN or PAM, primarily governs these two properties of the composite films.

### Mechanism of improvement of tensile properties of PAM/TOCN composite films

The aqueous 0.15 % PAM-COONa solution and 0.15 % TOCN-COONa dispersion both had pHs of ∼7, and the aqueous 0.15 % PAM-COOH solution and 0.15 % TOCN-COOH dispersion both had pHs of ∼4. The PAM-COONa and TOCN-COONa used in this study had similar charge densities of approximately −1 meq/g in water at pH ∼7, and those of the PAM-COOH and TOCN-COOH were approximately −0.65 meq/g in water at pH ∼4. The anionic charge densities of (PAM/TOCN)-H were therefore ∼65 % those of (PAM/TOCN)-Na in aqueous mixtures. However, the primary factor in increasing the Young's moduli and tensile strengths of the composite films was the PAM content, for both the (PAM/TOCN)-Na and (PAM/TOCN)-H composite films. The difference in the charge density between (PAM/TOCN)-Na and (PAM/TOCN)-H in aqueous mixtures therefore had almost no influence on the tensile properties of the dried composite films. The counter ion of the carboxyl groups (i.e., either sodium carboxylate groups or protonated carboxyl groups) of the composite films also had no influence on their tensile properties.

Figure 6 shows FT-IR spectra of the (PAM/TOCN)-H films with different PAM contents. As shown in Fig. 1, the amide C=O and amide NH bands of PAM appeared at 1676 and 1616 cm$^{-1}$, respectively (Yan et al. 1998; Freddi et al. 1999). The protonated carboxyl groups of TOCN-COOH had an absorption band at 1723 cm$^{-1}$, from C=O stretching, and hydrogen boning can occur between two carboxyl groups (Fujisawa et al. 2011). The carboxyl C=O band of TOCN-COOH and the amide C=O band of PAM-COOH shifted to lower wavenumbers for the composite films, whereas the amide NH band of PAM-COOH was almost unchanged for all the films. These
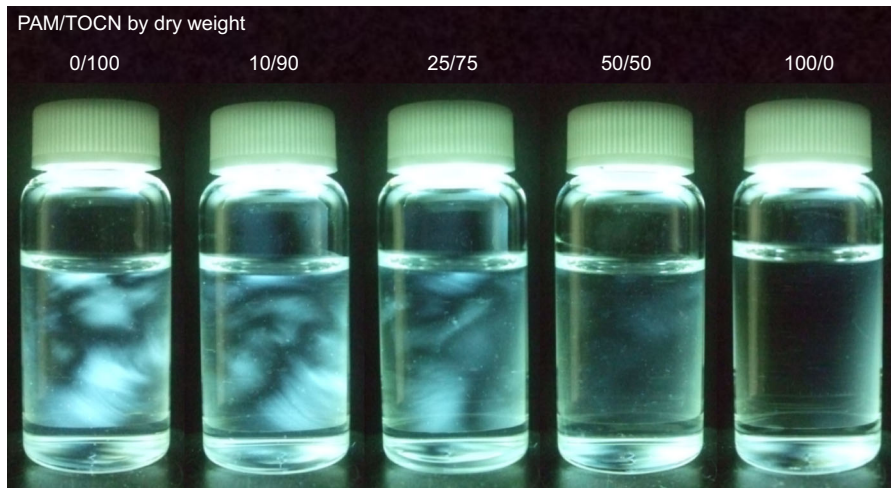
**Fig. 7** Photographs of aqueous (PAM/TOCN)-H mixtures (0.15 % solid content) taken between cross-polarizers

**Fig. 8** Schematic diagram of mechanism of improvement of tensile properties of PAM/TOCN composite films at 25 % PAM content
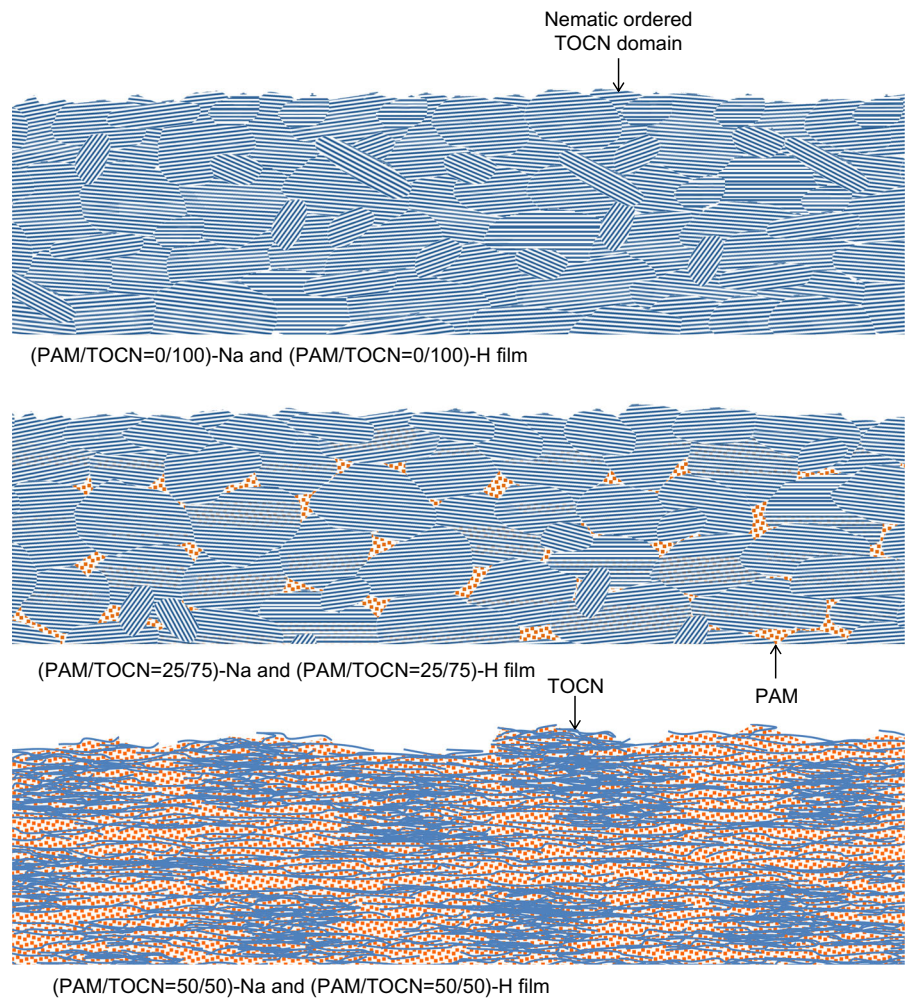
results show that the protonated carboxyl groups in TOCN-COOH formed stronger hydrogen bonds with amide C=O groups (Smith et al. 1992; Sun et al. 1993). However, these C=O band shifts cannot be directly correlated with the tensile properties observed in Figs. 4 and 5; the Young's moduli and tensile strengths of the TOCN-COOH films increased at 10–25 % PAM contents, but decreased at 50 % PAM content.

Saito et al. (2011) reported that TOCNs are individually nanodispersed in water, forming TOCN elements with self-aligned and nematic-ordered structures inside small domains (or clusters), as a result of electrostatic repulsion between anionically charged TOCN elements, although the domains are distributed randomly (or no ordered structures exist between the TOCN domains). As a result, the TOCN films prepared from aqueous TOCN dispersions by casting and drying have plywood-like layered structures with extremely high oxygen-barrier properties under dry conditions. The reported results and those obtained in this study suggest that the PAM molecules may play a role in repairing or filling defects present around the boundary region of the self-aligned TOCN domains in the composite films when the PAM contents are in the range 10–25 %.

When the aqueous 0.15 % (PAM/TOCN)-H mixtures were observed between cross-polarizers, the mixtures at PAM/TOCN weight ratios of 0/100, 10/90, and 25/75 showed clear birefringence, indicating the formation of TOCN elements with self-aligned and nematic-ordered structures in these mixtures (Fig. 7). In contrast, the aqueous mixtures at PAM/TOCN weight ratios of 50/50 and 100/0 showed nearly no birefringence. These results indicate that the nematic-ordered domain structures of TOCN elements, which give the TOCn films good tensile properties, were retained in aqueous mixtures with 0–25 % PAM contents (Saito et al. 2011).

A similar explanation is used for the nano-reinforcement effect of nanoclay/TOCN composite films (Wu et al. 2012, 2014), and therefore these effects are characteristic of TOCNs, which form self-aligned and nematic-ordered domain structures in aqueous dispersions. A schematic diagram of the mechanism of the improvement of the tensile properties of PAM/TOCN = 25/75 composite films is shown in Fig. 8. In the aqueous PAM/TOCN mixture with a weight ratio of 50/50, the TOCN domains originally present in the 100 % TOCN-COOH dispersion are mostly destroyed by diluting with the aqueous PAM-COOH solution, probably resulting in a structure similar to that of the PAM/TOCN = 50/50 composite film, shown at the bottom of Fig. 8. This hypothesis regarding the mechanism of improvement of the tensile properties of composite films by addition of 10–25 % PAM to TOCN consistently explains the obtained results.

## Conclusion

PAMs have the potential to reinforce TOCN films, irrespective of the sodium carboxylate groups or protonated carboxyl groups of TOCN or PAM, when the PAM content is in the range of 10–25 %. The Young's modulus and tensile strength of the 100 % TOCN film clearly increase at these PAM contents. The FT-IR spectra of the (PAM/TOCN)-H films with various PAM/TOCN weight ratios indicate the formation of hydrogen bonds between protonated carboxyl groups of TOCN-COOH and amide C=O groups of PAM-COOH. However, the formation of these hydrogen bonds does not rationally explain the reinforcing effect achieved by PAM addition to TOCN-COOH. Because the TOCN elements form self-aligned and nematic-ordered domain structures in aqueous dispersion, the PAM molecules at these contents are probably present around the boundary regions of TOCN domains or between the TOCN domains, and fill or cover defects (or discontinuous regions) that cause deteriorations in the mechanical properties. The formation of nematic-ordered domain structures of TOCNs in aqueous dispersions therefore probably plays a significant role in the reinforcing effects achieved by the addition of water-soluble PAM molecules.

## References

Chen J, Heitmann JA, Hubbe MA (2003) Dependency of polyelectrolyte complex stoichiometry on the order of addition. 1. Effect of salt concentration during streaming current titrations with strong polyacid and polybase. Colloids Surf A 223:215–230

Endo R, Saito T, Isogai A (2013) TEMPO-oxidized cellulose nanofibril/poly(vinyl alcohol) composite drawn fibers. Polymer 54:935–941

Freddi G, Tsukada M, Beretta S (1999) Structure and physical properties of silk fibroin/polyacrylamide blend films. J Appl Polym Sci 71:1563–1571

Fujisawa S, Okita Y, Fukuzumi H, Saito T, Isogai A (2011) Preparation and characterization of TEMPO-oxidized cellulose nanofibrils films with free carboxyl groups. Carbohydr Polym 84:579–583

Fukuzumi H, Saito T, Iwata T, Kumamoto Y, Isogai A (2009) Transparent and high gas barrier films of cellulose nanofibers prepared by TEMPO-mediated oxidation. Biomacromolecules 10:162–165

Fukuzumi H, Fujisawa S, Saito T, Isogai A (2013) Selective permeation of hydrogen gas using cellulose nanofibril film. Biomacromolecules 14:1705–1709

Henriksson M, Berglund LA, Isaksson P, Lindström T, Nishino T (2008) Cellulose nanopaper structures of high toughness. Biomacromolecules 9:1579–1585

Hiraoki R, Ono Y, Saito T, Isogai A (2015) Molecular mass and molecular-mass distribution of TEMPO-oxidized celluloses and TEMPO-oxidized cellulose nanofibrils. Biomacromolecules 16:675–681

Homma I, Fukuzumi H, Saito T, Isogai A (2013) Effects of carboxyl-group counter-ions on biodegradation behaviors of TEMPO-oxidized cellulose fibers and nanofibrils films. Cellulose 20:2505–2515

Isogai A (2013) Wood nanocelluloses: fundamentals and applications as new bio-based nanomaterials. J Wood Sci 59:449–459

Isogai A, Saito T, Fukuzumi H (2011) TEMPO-oxidized cellulose nanofibers. Nanoscale 3:71–85

Johnson RK, Zink-Sharp A, Renneckar SH, Glasser WG (2009) A new bio-based nanocompoiste: fibrillated TEMPO-oxidized celluloses in hydroxypropylcellulose matrix. Cellulose 16:227–238

Klemm D, Kramer F, Moritz S, Lindström T, Ankerfors M, Gray D, Dorris A (2011) Nanocelluloses: a new family of nature-based materials. Angew Chem Int Ed 50:5438–5466

Kurihara T, Isogai A (2014) Properties of poly(acrylamide)/TEMPO-oxidized cellulose nanofibril composite films. Cellulose 21:291–299

Kurihara T, Isogai A (2015) The effect of electric charge density of polyacrylamide (PAM) on properties of PAM/cellulose nanofibril composite films. Cellulose 22:499–506

Liu A, Walther A, Ikkala O, Belova L, Berglund LA (2011) Clay nanopaper with tough cellulose nanofiber matrix for fire retardancy and gas barrier functions. Biomacromolecules 12:633–641

Saito T, Kimura S, Nishiyama Y, Isogai A (2007) Cellulose nanofibers prepared by TEMPO-mediated oxidation of native cellulose. Biomacromolecules 8:2485–2491

Saito T, Uematsu T, Kimura S, Enomae T, Isogai A (2011) Self-aligned integration of native cellulose nanofibrils towards producing diverse bulk materials. Soft Matter 7:8804–8809

Sehaqui H, Liu A, Zhou Q, Berglund LA (2010) Fast preparation procedure for large, flat cellulose and cellulose/inorganic nanopaper structures. Biomacromolecules 11:2195–2198

Sehaqui H, Zhou Q, Berglund LA (2011) Nanostructured bio-composites of high toughness—a wood cellulose nanofiber network in ductile hydroxyethylcellulose matrix. Soft Matter 7:7342–7350

Shimizu M, Fukuzumi H, Saito T, Isogai A (2013) Preparation and characterization of TEMPO-oxidized cellulose-nanofibrils with ammonium carboxylate groups. Int J Biol Macromol 59:99–104

Shimizu M, Saito T, Isogai A (2014a) Bulky quaternary alkylammonium counterions enhance the nanodispersibility of 2,2,6,6-tetramethylpiperidine-1-oxyl-oxidized cellulose in diverse solvents. Biomacromolecules 15:1904–1909

Shimizu M, Saito T, Fukuzumi H, Isogai A (2014b) Hydrophobic, ductile, and transparent nanocellulose films with quaternary alkylammonium carboxylates on nanofibril surfaces. Biomacromolecules 15:4320–4325

Shinoda R, Saito T, Okita Y, Isogai A (2012) Relationship between length and degree of polymerization of TEMPO-oxidized cellulose nanofibrils. Biomacromolecules 13:842–849

Smith EL, Alves CA, Anderegg JW, Porter MD, Siperko LM (1992) Deposition of metal overlayers at end-group-functionalized thiolate monolayers adsorbed at gold. 1. Surface and interfacial chemical characterization of deposited copper overlayers at carboxylic acid-terminated structures. Langmuir 8:2707–2714

Sun L, Crooks RM, Ricco AJ (1993) Molecular interactions between organized, surface-confined monolayers and vapor-phase probe molecules. 5. Acid-base interactions. Langmuir 9:1775–1780

Takahashi M, Iyoda K, Miyauchi T, Ohkido S, Tahashi M, Wakita K, Kajitani N, Kurachi M, Hotta K (2009) Preparation and characterization of Eu: Ti codoped LiNbO$_3$ films prepared by the sol–gel method. J Appl Phys 106:044102

Wu CN, Saito T, Fujisawa S, Fukuzumi H, Isogai A (2012) Ultrastrong and high gas-barrier nanocellulose/clay-layered composites. Biomacromolecules 13:1927–1932

Wu CN, Yang Q, Takeuchi M, Saito T, Isogai A (2014) Highly tough and transparent layered composites of nanocellulose and synthetic silicate. Nanoscale 6:392–399

Yan F, Zheng C, Zhai X, Zhao D (1998) Preparation and characterization of polyacrylamide in cationic microemulsion. J Appl Polym Sci 67:747–754